

The Oncogene ECT2 Contributes to a Hyperplastic, Proliferative Lung Epithelial Cell Phenotype in Idiopathic Pulmonary Fibrosis

Henrik M. Ulke¹, Kathrin Mutze¹, Mareike Lehmann¹, Darcy E. Wagner^{1,2}, Katharina Heinzlmann¹, Andreas Günther³, Oliver Eickelberg⁴, and Melanie Königshoff^{1,4}

¹Lung Repair and Regeneration, Comprehensive Pneumology Center, Ludwig Maximilians University, University Hospital Großhadern, and Helmholtz Zentrum München, Member of the German Center for Lung Research, Munich, Germany; ²Lung Bioengineering and Regeneration, Lund University, Lund, Sweden; ³Department of Internal Medicine, Universities of Giessen and Marburg Lung Center, Justus Liebig University Giessen, Member of the German Center for Lung Research, Giessen, Germany; and ⁴Division of Pulmonary Sciences and Critical Care Medicine, Department of Medicine, University of Colorado, Denver, Aurora, Colorado

ORCID IDs: 0000-0003-3794-1309 (D.E.W.); 0000-0002-6904-4904 (K.H.); 0000-0001-7170-0360 (O.E.).

Abstract

Idiopathic pulmonary fibrosis (IPF) and lung cancer are progressive lung diseases with a poor prognosis. IPF is a risk factor for the development of lung cancer, and the incidence of lung cancer is increased in patients with IPF. The disease pathogenesis of IPF and lung cancer involves common genetic alterations, dysregulated pathways, and the emergence of hyperplastic and metaplastic epithelial cells. Here, we aimed to identify novel, common mediators that might contribute to epithelial cell reprogramming in IPF. Gene set enrichment analysis of publicly available non-small cell lung cancer and IPF datasets revealed a common pattern of misregulated genes linked to cell proliferation and transformation. The oncogene *ECT2* (epithelial cell transforming sequence 2), a guanine nucleotide exchange factor for Rho GTPases, was highly enriched in both IPF and non-small cell lung cancer compared with nondiseased controls.

Increased expression of *ECT2* was verified by qPCR and Western blotting in bleomycin-induced lung fibrosis and human IPF tissue. Immunohistochemistry demonstrated strong expression of *ECT2* staining in hyperplastic alveolar epithelial type II (ATII) cells in IPF, as well as its colocalization with proliferating cell nuclear antigen, a well-known proliferation marker. Increased *ECT2* expression coincided with enhanced proliferation of primary mouse ATII cells as analyzed by flow cytometry. *ECT2* knockdown in ATII cells resulted in decreased proliferation and collagen I expression *in vitro*. These data suggest that the oncogene *ECT2* contributes to epithelial cell reprogramming in IPF, and further emphasize the hyperplastic, proliferative ATII cell as a potential target in patients with IPF and lung cancer.

Keywords: alveolar epithelial cells; oncogenic pathways; lung fibrosis; gene set enrichment analysis; lung cancer

Idiopathic pulmonary fibrosis (IPF) and lung cancer are two chronic, progressive, and fatal lung diseases that cause extensive destruction of lung structure and thus function. For both diseases, only limited

treatment options are available, leading to high mortality and highly reduced survival rates (overall 5-yr survival rate of 20–30% for IPF [1] and 18% for lung cancer [2]). The pathogenesis of IPF and lung cancer

has often been associated with common risk factors such as cigarette smoke (3–5) and age (2, 6, 7). Over the past few years, an increasing number of publications have described lung cancer as a frequent

(Received in original form February 11, 2019; accepted in final form May 30, 2019)

Supported by the Helmholtz Association, German Center for Lung Research (HGF-W2/W3-022). D.E.W. was supported by a Whitaker International Scholar Fellowship and the Helmholtz Munich Postdoctoral Program.

Author Contributions: H.M.U., K.M., O.E., and M.K. designed and supervised the project. H.M.U., K.M., and M.L. performed the experiments. H.M.U., K.M., M.L., D.E.W., A.G., and O.E. analyzed and interpreted the results. H.M.U., K.H., and M.K. prepared the manuscript. All authors critically revised the manuscript. M.K. is the guarantor of this work and as such had full access to all the data in the study and takes responsibility for the integrity of the data and the accuracy of the data analysis.

Correspondence and requests for reprints should be addressed to Melanie Königshoff, M.D., Ph.D., Division of Pulmonary Sciences and Critical Care Medicine, Department of Medicine, University of Colorado, Denver, Anschutz Medical Campus, Research 2, 9th Floor, 12700 East 19th Avenue, Aurora, CO 80045. E-mail: melanie.koenigshoff@ucdenver.edu.

This article has an online supplement, which is accessible from this issue's table of contents at www.atsjournals.org.

Am J Respir Cell Mol Biol Vol 61, Iss 6, pp 713–726, Dec 2019

Copyright © 2019 by the American Thoracic Society

Originally Published in Press as DOI: 10.1165/rcmb.2019-0047OC on May 30, 2019

Internet address: www.atsjournals.org

comorbidity of patients with IPF, with a prevalence ranging from 3% to 48% (8–11) (this discrepancy in prevalence may be due to differences in the elapsed time after IPF diagnosis and the study designs used). These studies have been complemented by multiple studies reporting that the cumulative incidence of lung cancer in patients with IPF is dramatically increasing in follow-up examinations, i.e., from 12.2% (5 yr) to 23.3% (10 yr) (9), 41% (1 yr) to 82% (3 yr) (11), and 3.3% (1 yr) to 15.4% (5 yr) to 54.7% (10 yr) (12). The predominant histological subtype of lung cancer observed in IPF is non-small cell lung cancer (NSCLC) in the form of adenocarcinoma or squamous cell carcinoma, which are mainly located in the lower peripheral lobes of IPF lungs adjacent to areas of fibrosis and honeycombing (9, 11, 13–15). Moreover, patients with combined IPF and lung cancer have a significantly shorter survival time than patients with only IPF (10, 11), and have an increased probability to develop significant complications such as acute exacerbations and pneumonia after surgical treatment, chemotherapy, and radiotherapy (16, 17). Thus, there is an urgent need to determine whether IPF and NSCLC share common pathomechanistic features, which could lead to the identification of novel therapeutic targets.

Current evidence suggests that lung epithelial cell injury and reprogramming (18) are central drivers of IPF and are accompanied by fibroblast activation and immune cell dysfunction, which leads to altered extracellular matrix (ECM) deposition and lung remodeling (19, 20). Epithelial cell reprogramming resembles a variety of different phenotypes, such as bronchial and alveolar epithelial type II (ATII) cell hyperplasia and squamous metaplasia, which are frequently observed in areas of lung fibrosis or honeycombing (21) and may represent hotspots for the development of lung cancer (22). More recently, it has been reported that IPF and lung cancer may share common mechanisms, such as epigenetic alterations (23) and microsatellite instability and loss of heterozygosity (24), as well as dysregulated signaling pathways (25). Thus, we hypothesized that the upregulation of cancer-related genes in IPF contributes to adaptive processes of epithelial cells, such as epithelial cell reprogramming and phenotype switching in IPF.

In this study, using an unbiased approach to find novel therapeutic targets for IPF/NSCLC, we identified the ECT2 (epithelial cell transforming sequence 2) oncogene as a potential mediator of epithelial cell reprogramming. ECT2 is a guanine nucleotide exchange factor (GEF) for the Rho GTPases family (26). Increased expression of ECT2 has been shown in different tumor types, including NSCLC, where it was related to a poor overall prognosis, increased tumor growth, and invasion (27, 28). Here, we investigated the potential contribution of ECT2 to the pathogenesis of epithelial cell reprogramming in IPF.

Some of the results of these studies have been previously reported in the form of an abstract at the American Thoracic Society 2017 International Conference (29).

Methods

For a detailed description of the materials and methods used in this work, please refer to the data supplement.

Analysis of Public Microarray and RNA Sequencing Datasets

Public microarray and RNA sequencing data were retrieved from the Gene Expression Omnibus (30) (<https://www.ncbi.nlm.nih.gov/geo/>; National Center for Biotechnology Information) and the European Nucleotide Archive (31) (<https://www.ebi.ac.uk/ena/>; European Molecular Biology Laboratory–European Bioinformatics Institute). The data are available through accession numbers GSE47460 (32, 33), GSE32537 (34), GSE44077 (35), GSE43458 (36), GSE18842 (37), GSE10921 (38), and GSE94555 (PRJNA371464/SRP098915) (39). When necessary, microarray data were background corrected, normalized, and log₂ transformed. Differentially expressed genes (DEGs) were defined by a log₂ fold change > 1.0 and adjusted *P* value < 0.05.

Gene set enrichment analysis (GSEA) was performed and the enrichment of a gene set in one distinct phenotype was deemed significant with a false discovery rate (FDR) *q* value < 0.05 and a nominal *P* value < 0.05. Subsequently, a functional annotation analysis was performed. Pathways were considered to be significantly enriched with a Benjamini

and Hochberg FDR of <0.05 and more than two genes of the respective pathway present in the analyzed gene set. Gene Ontology (GO) concepts were considered significantly enriched with an FDR of <0.05 and two or more genes of the respective GO concept detected in the analyzed gene set.

Tissue Samples and Cells

Human tissue specimens collected by the European IPF Registry were provided by the Universities of Giessen and Marburg Lung Center Biobank, a member of the German Center for Lung Research Platform Biobank. The study protocol was approved by the ethics committee of the Medical Department of Justus Liebig University (project no. 111/08 and 58/15). Written informed consent was provided by all subjects included in this study. For animal experiments, pathogen-free, 6- to 8-week-old female C57BL/6N mice (Charles River Laboratories) were used. Experimental lung fibrosis was induced by a single intratracheal administration of 2 U/kg body weight bleomycin (Bleo) sulfate (Sigma-Aldrich) with a MicroSprayer Aerosolizer (model IA-1C; Penn Century). Animal experiments were performed in accordance with the guidelines and regulations of the ethics committee of Helmholtz Zentrum München and approved by the Regierung von Oberbayern (AZ: 55.2-1-54-2532-88-2012).

Statistical Analysis

If not stated otherwise, statistical analysis was performed using GraphPad Prism v5 software (GraphPad Software). An unpaired *t*-test (two-tailed) or paired *t*-test (two-tailed) was used for analysis comparing two groups, as stated in the figure legends. Multiple groups were compared using one-way ANOVA with Bonferroni's multiple-comparison post test. Correlation was analyzed with the Pearson's test. Data are shown as mean ± SD. A *P* value < 0.05 was considered statistically significant (**P* < 0.05, ***P* < 0.01, and ****P* < 0.001).

Results

GSEA Identifies a Pattern of Commonly Upregulated Genes in IPF and NSCLC

To examine a possible connection between IPF/NSCLC and gene expression levels, we

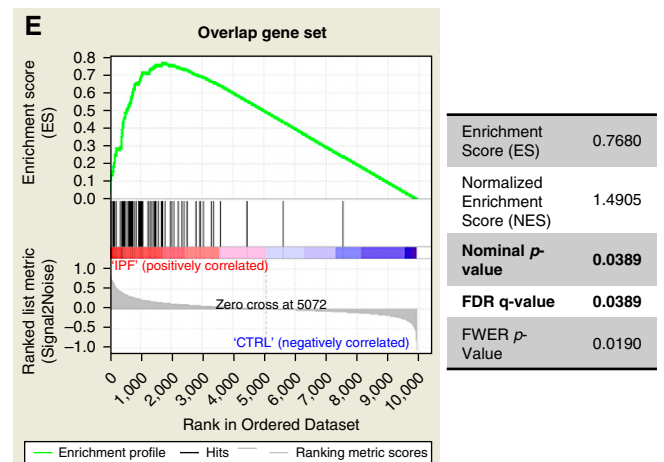
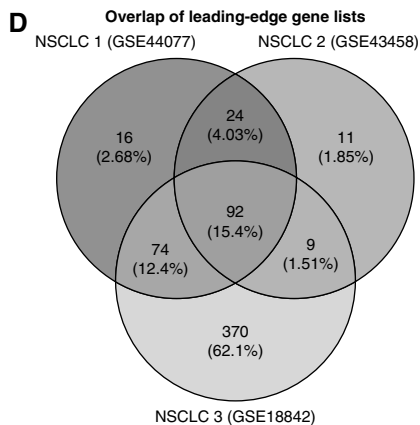
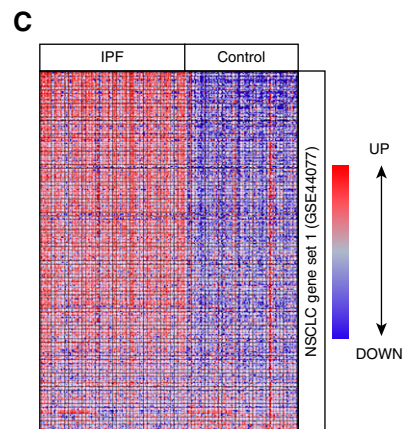
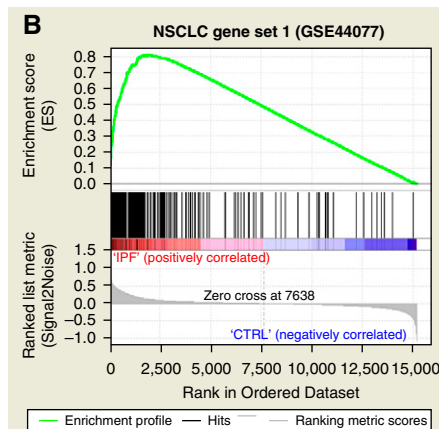
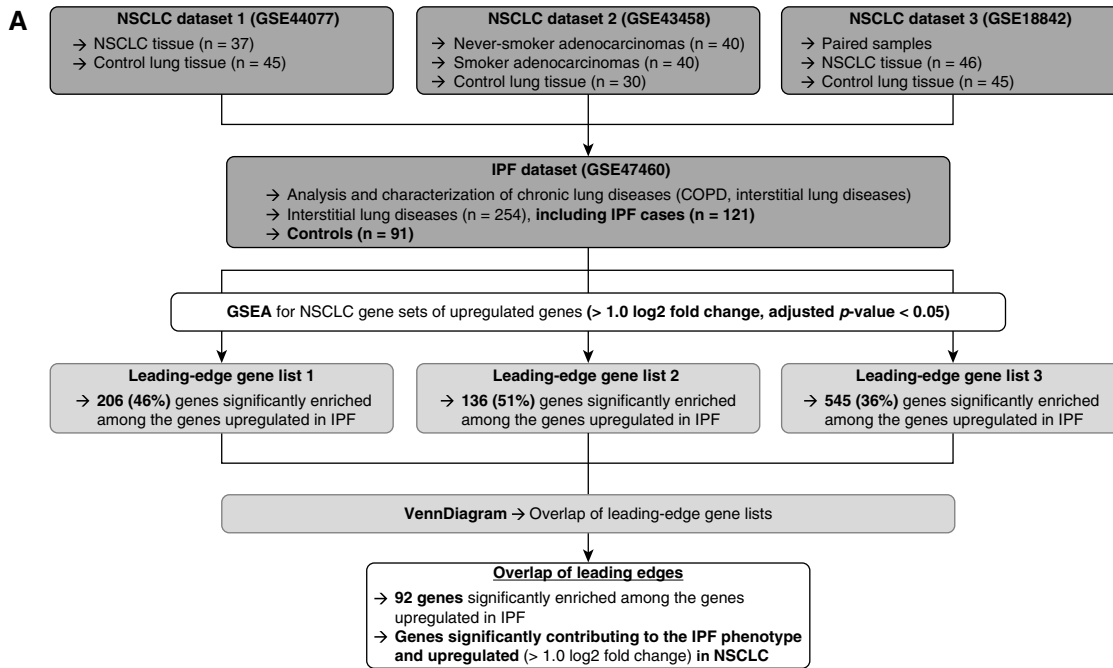


Figure 1. Gene set enrichment analysis (GSEA) reveals a common pattern of upregulated genes in non-small cell lung cancer (NSCLC) and idiopathic pulmonary fibrosis (IPF). (A) Schematic overview illustrating the workflow for generating the gene list of 92 genes upregulated in NSCLC (>1.0 log₂ fold change, adjusted P value < 0.05) and significantly enriched among genes upregulated in the IPF phenotype, by three independent GSEA runs (datasets: GSE47460, GSE44077, GSE43458, and GSE18842). The number of cases is indicated. (B) Left: representative enrichment plot showing the results for

used GSEA to compare misregulated genes in both diseases and thereby evaluate common patterns (Figure 1A). We analyzed three independent and previously described NSCLC microarray datasets (GSE44077, GSE43458, and GSE18842) for DEGs in subjects with NSCLC compared with nondiseased control subjects, focusing on upregulated genes. The corresponding gene sets are referred to as NSCLC gene set 1 (GSE44077, $n = 449$), NSCLC gene set 2 (GSE43458, $n = 268$), and NSCLC gene set 3 (GSE18842, $n = 1,520$). A microarray dataset of chronic lung diseases (GSE47460), including IPF ($n = 121$) and control ($n = 91$) cases, was used for GSEA. Subsequently, NSCLC gene sets 1–3 were each included in the GSEA. We found a significant enrichment (FDR q value < 0.05 ; nominal P value < 0.001) of all three NSCLC gene sets in the IPF phenotype (Figure 1B and Figures E1A and E1B in the data supplement). Clustering of the DEGs (NSCLC gene set 1, GSE44077) in either the IPF or control group by their respective expression levels in the GSE47460 microarray dataset is visualized as a heatmap in Figure 1C. Based on the GSEA, we created three leading-edge (LE) gene lists representing the genes that contributed the most to the enrichment of the respective gene set within the GSEA and therefore are targets of high interest (40). We further analyzed these LE gene lists for their overlap (the results are presented as a Venn diagram in Figure 1D) and found that 92 genes were upregulated in all three NSCLC microarray datasets (\log_2 fold change > 1.0 and adjusted P value < 0.05) and enriched in IPF. Moreover, we confirmed the differential expression of these genes in another independent IPF dataset (GSE32537), further indicating that this subset of genes might play an important role in the pathogenesis of IPF (Figure 1E).

The Overlap Gene Set Reveals an ATII Cell Signature and Is Significantly Enriched in Processes Associated with Cell Proliferation

Next, we asked whether the Overlap gene set was enriched in a specific cell type of IPF lungs. Using GSEA, we compared this gene set of interest with microarray or RNA-sequencing datasets from human fibroblasts from IPF and control lungs (GSE10921), human ATII cells from IPF and control lungs (GSE94555), and primary mouse ATII (pmATII) cells from Bleo-induced experimental lung fibrosis and control mice (41). Our gene set of interest showed a strong enrichment in fibrotic lung epithelial cells within the IPF and Bleo-induced lung fibrosis datasets (FDR q value < 0.001 ; nominal P value < 0.001) (Figure 2A).

Next, we performed a functional annotation analysis using the Kyoto Encyclopedia of Genes and Genomes (KEGG) and REACTOME pathway databases. KEGG pathway enrichment analysis revealed a significant enrichment of five distinct pathways (Table 1), including cell cycle, progesterone-mediated oocyte maturation, cellular senescence, oocyte meiosis, and the p53 signaling pathway. REACTOME pathway enrichment analysis showed a significant enrichment of 67 pathways, most of which were associated with either cell proliferation or the ECM (Table 2). GO enrichment analysis further underlined a strong proliferative phenotype (Table 3), and the top enriched GO concepts are color coded in Figure 2B. Potential protein interactions are demonstrated in a STRING protein–protein interaction network (Figure 2B).

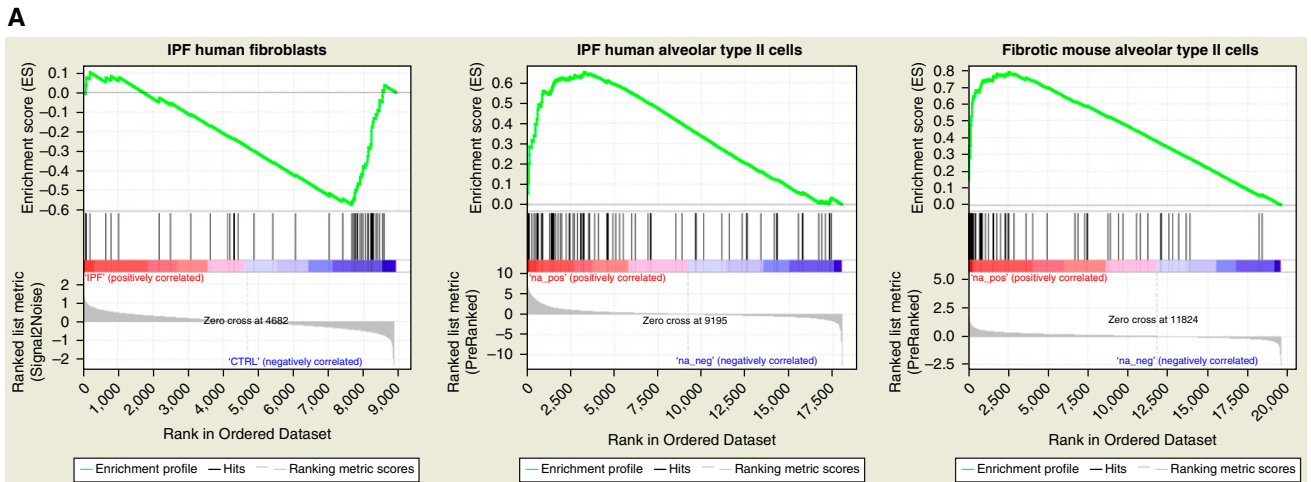
The Oncogene ECT2 Is Upregulated in ATII Cells from Experimental and Human Lung Fibrosis

The oncogene ECT2 was identified among the genes of the Overlap gene set and was

also one of the top LE genes in the GSEA of fibrotic pmATII cells (Figure 2A, right enrichment plot). Moreover, the transcript levels of *Ect2* showed that it was among the top upregulated genes in an unbiased microarray dataset comparing fibrotic and healthy pmATII cells (Figure 3A; log-fold change *Ect2*: 1.18 ± 0.45) (41). ECT2 is a GEF for the Rho family GTPases Cdc42, Rac1, and RhoA, and thus has been implicated in cell cycle regulation and proliferation (26)—processes that are known to be impaired in lung fibrosis (18, 41). Based on these observations, we aimed to further investigate the role of ECT2 in epithelial cell reprogramming in lung fibrosis. First, *Ect2* upregulation was confirmed by qRT-PCR (Figure 3B; $\Delta\text{Ct } Ect2$: PBS -2.00 ± 1.22 vs. Bleo 0.34 ± 0.88 ; $***P < 0.001$) and on the protein level by Western blotting (Figures 3D and 3E; relative protein level ECT2: PBS 0.07 ± 0.05 vs. Bleo 0.48 ± 0.20 ; $**P < 0.01$). In contrast, *Ect2* mRNA levels were unchanged between whole-lung homogenates from Bleo- and PBS-treated mice (Figure 3C; $\Delta\text{Ct } Ect2$: PBS -4.50 ± 0.52 vs. Bleo -4.14 ± 0.72 ; nonsignificant). To further assess the main cell type that highly expressed ECT2 in pulmonary fibrosis *in situ*, we performed immunohistochemical stainings of ECT2 in lung tissue sections derived from Bleo- and PBS-treated mice. ECT2 was mainly found in the alveolar epithelium and was highly enriched in fibrotic tissue (Figure 3F, black arrows).

We further validated the upregulation of ECT2 in IPF lung tissue specimens using a published IPF microarray dataset (GSE47460) (Figure 4A; log₂-based gene expression levels ECT2: donor 6.40 ± 0.57 vs. IPF 6.97 ± 0.37 ; $***P < 0.001$), and qRT-PCR in whole-lung homogenates from IPF versus donor lung tissue specimens from an independent cohort

Figure 1. (Continued). one GSEA run; IPF dataset and phenotypes (GSE47460) together with the NSCLC gene set 1 (GSE44077) (upregulated genes only; >1.0 log₂ fold change; adjusted P value < 0.05 ; $n = 449$). Right: statistically significant enrichment of the NSCLC gene set 1 within the IPF phenotype (false discovery rate [FDR] q value < 0.05 ; nominal P value < 0.001). Additional enrichment plots are provided in Figure E1. (C) Heatmap generated by GSEA showing a clear separation of genes from the NSCLC gene set 1 (GSE44077) toward the IPF or control phenotype. (D) Venn diagram generated from the three leading-edge gene lists. The total number of genes applied from the three gene lists was set as 100%. The number of genes is indicated. The central overlap of 92 genes (15.4%) was extracted and is referred to as the Overlap gene set. (E) Enrichment plot for the confirmatory GSEA run; IPF dataset with phenotypes (GSE32537) and the Overlap gene set ($n = 92$). The Overlap gene set is significantly enriched in the IPF phenotype (FDR q value < 0.05 ; nominal P value < 0.05) of an additional and independent IPF cohort. COPD = chronic obstructive pulmonary disease; CTRL = control; FWER = family-wise error rate.



Dataset and phenotypes	Gene set	Enrichment Score (ES)	Normalized Enrichment Score (NES)	Nominal <i>p</i> -value	FDR <i>q</i> -value	FWER <i>p</i> -Value
IPF human fibroblasts (GSE10921)	Overlap	-0.5760	-2.2948	< 0.001	< 0.001	< 0.001
IPF human alveolar type II cells (GSE94555)	Overlap	0.6519	1.8353	< 0.001	< 0.001	< 0.001
Mouse fibrotic alveolar type II cells (41)	Overlap	0.7876	2.3798	< 0.001	< 0.001	< 0.001

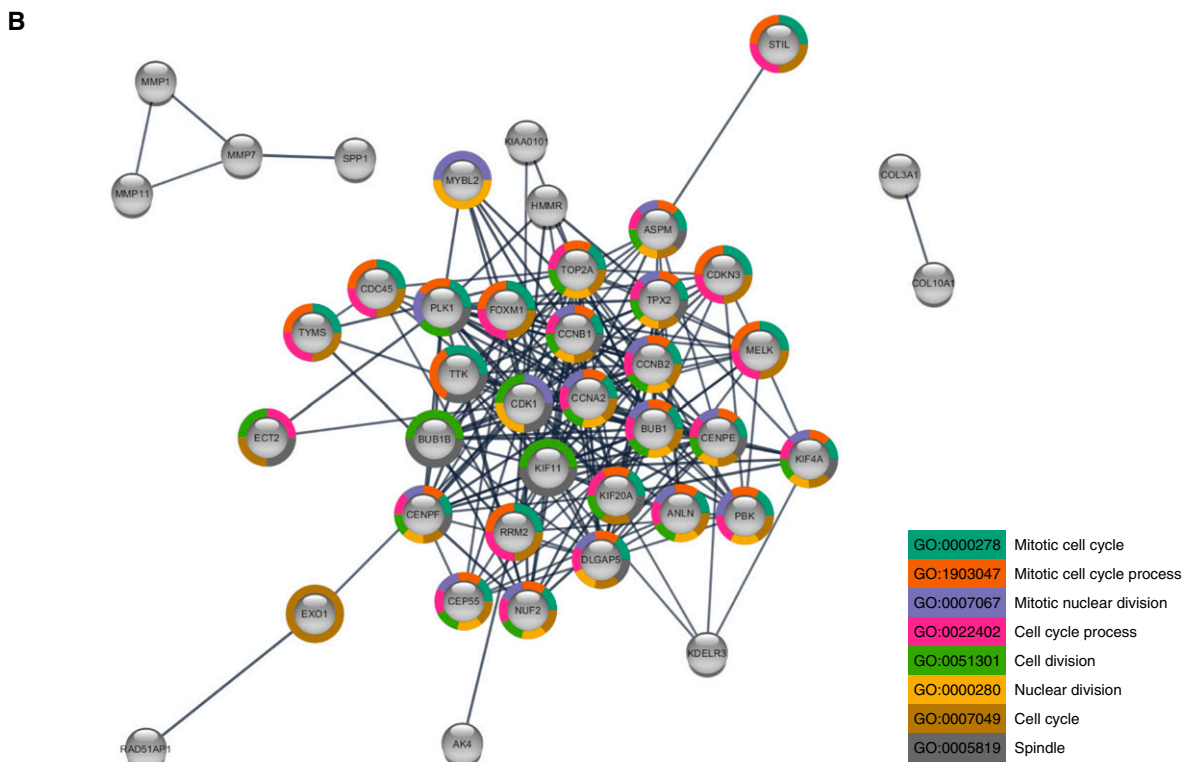


Figure 2. Overlap of leading-edge gene lists reveals an alveolar epithelial cell signature and is significantly enriched in biological processes associated with cell proliferation. (A) Enrichment plots for three independent GSEA runs. The Overlap gene set ($n = 92$) showed significant enrichment (FDR q value < 0.001; nominal P value < 0.001) in the control phenotype of an IPF human fibroblast dataset (GSE10921) and in the fibrotic phenotype of IPF human and murine alveolar epithelial type II (ATII) cell datasets (GSE94555; primary mouse ATII [pmATII] [41]). (B) The STRING protein-protein interaction (PPI) network (confidence score cutoff > 0.9) generated from the Overlap gene set (nodes = 90; edges = 210) showed significant PPI enrichment (PPI enrichment P value < 1.0×10^{-16}). Only connected nodes are displayed ($n = 42$). Gene ontology (GO) enrichment analysis revealed significant enrichment (FDR < 0.05 and two or more detected genes) in 171 GO concepts. The top eight GO concepts are color coded.

Table 1. KEGG Pathway Enrichment Analysis for the Overlap Gene Set

Pathway	ID	FDR	P Value	Genes
Cell cycle	hsa04110	1.81E-06	1.62E-08	PLK1, BUB1, BUB1B, TTK, CDC45, CCNA2, CCNB1, CCNB2, CDK1
Progesterone-mediated oocyte maturation	hsa04914	0.0007	1.18E-05	PLK1, BUB1, CCNA2, CCNB1, CCNB2, CDK1
Cellular senescence	hsa04218	0.0058	0.0002	FOXM1, MYBL2, CCNA2, CCNB1, CCNB2, CDK1
Oocyte meiosis	hsa04114	0.0091	0.0004	PLK1, BUB1, CCNB1, CCNB2, CDK1
p53 signaling pathway	hsa04115	0.0091	0.0004	RRM2, CCNB1, CCNB2, CDK1

Definition of abbreviations: FDR = false discovery rate; KEGG = Kyoto Encyclopedia of Genes and Genomes.

(Figure 4B; Δ Ct *ECT2*: donor 2.95 ± 0.82 vs. IPF 4.82 ± 1.58 ; $*P < 0.05$). Notably, *ECT2* mRNA levels were found to be significantly increased in microdissected alveolar septae and primary ATII cells from human IPF lungs compared with donor lungs (Figure 4C; Δ Ct *ECT2*: septae donor 1.87 ± 0.26 vs. IPF 2.80 ± 0.67 ; ATII donor 2.02 ± 0.31 vs. IPF 2.93 ± 0.62 ; $*P < 0.05$). Immunohistochemical stainings of *ECT2* in lung tissue from IPF and donor specimens showed *ECT2*⁺ staining almost exclusively in aberrant, hyperplastic alveolar epithelial cells in IPF sections, and there was no or only rare *ECT2* staining in lung sections from donor specimens (Figure 4D). Together, these data show that ATII cells are one of the main sources for *ECT2* expression in pulmonary fibrosis.

Table 2. Top 20—REACTOME Pathway Enrichment Analysis for the Overlap Gene Set

Pathway	ID	FDR	P value	Genes
Cell cycle, mitotic	R-HSA-69278	4.06E-10	1.27E-12	BUB1, BUB1B, CCNA2, CCNB1, CCNB2, CDC45, CDK1, CENPE, CENPF, FOXM1, HMMR, KIF20A, MYBL2, NUF2, PLK1, RRM2, TOP2A, TPX2, TYMS
Cell cycle	R-HSA-1640170	6.73E-10	4.19E-12	BUB1, BUB1B, CCNA2, CCNB1, CCNB2, CDC45, CDK1, CENPE, CENPF, EXO1, FOXM1, HMMR, KIF20A, MYBL2, NUF2, PLK1, RRM2, TOP2A, TPX2, TYMS
Polo-like kinase-mediated events	R-HSA-156711	5.88E-08	5.49E-10	CCNB1, CCNB2, CENPF, FOXM1, MYBL2, PLK1
Resolution of sister chromatid cohesion	R-HSA-2500257	2.43E-07	3.03E-09	BUB1, BUB1B, CCNB1, CCNB2, CDK1, CENPE, CENPF, NUF2, PLK1
Cyclin A/B1/B2-associated events during G2/M transition	R-HSA-69273	3.37E-07	5.25E-09	CCNA2, CCNB1, CCNB2, CDK1, FOXM1, PLK1
Cell cycle checkpoints	R-HSA-69620	3.87E-07	7.24E-09	BUB1, BUB1B, CCNA2, CCNB1, CCNB2, CDC45, CDK1, CENPE, CENPF, EXO1, NUF2, PLK1
G2/M transition	R-HSA-69275	8.13E-07	1.84E-08	CCNA2, CCNB1, CCNB2, CDK1, CENPF, FOXM1, HMMR, MYBL2, PLK1, TPX2
Mitotic G2-G2/M phases	R-HSA-453274	8.13E-07	2.03E-08	CCNA2, CCNB1, CCNB2, CDK1, CENPF, FOXM1, HMMR, MYBL2, PLK1, TPX2
Activation of NIMA kinases NEK9, NEK6, and NEK7	R-HSA-2980767	4.73E-06	1.33E-07	CCNB1, CCNB2, CDK1, PLK1
Mitotic prometaphase	R-HSA-68877	7.76E-06	2.42E-07	BUB1, BUB1B, CCNB1, CCNB2, CDK1, CENPE, CENPF, NUF2, PLK1
Mitotic G1-G1/S phases	R-HSA-453279	1.73E-05	5.91E-07	CCNA2, CCNB1, CDC45, CDK1, MYBL2, RRM2, TOP2A, TYMS
Golgi cisternae pericentriolar stack reorganization	R-HSA-162658	3.21E-05	1.20E-06	CCNB1, CCNB2, CDK1, PLK1
Collagen degradation	R-HSA-1442490	4.71E-05	1.91E-06	MMP1, MMP11, MMP12, MMP7, PRSS2
G2/M DNA replication checkpoint	R-HSA-69478	0.0001	5.12E-06	CCNB1, CCNB2, CDK1
M phase	R-HSA-68886	0.0001	5.61E-06	BUB1, BUB1B, CCNB1, CCNB2, CDK1, CENPE, CENPF, KIF20A, NUF2, PLK1
Amplification of signal from unattached kinetochores via a MAD2 inhibitory signal	R-HSA-141444	0.0001	6.59E-06	BUB1, BUB1B, CENPE, CENPF, NUF2, PLK1
Amplification of signal from the kinetochores	R-HSA-141424	0.0001	6.59E-06	BUB1, BUB1B, CENPE, CENPF, NUF2, PLK1
Phosphorylation of Emi1	R-HSA-176417	0.0001	7.65E-06	CCNB1, CDK1, PLK1
Extracellular matrix organization	R-HSA-1474244	0.0002	1.10E-05	COL10A1, COL3A1, ITGA11, MMP1, MMP11, MMP12, MMP7, PRSS2, SPP1
G0 and early G1	R-HSA-1538133	0.0002	1.18E-05	CCNA2, CDK1, MYBL2, TOP2A

Definition of abbreviations: Emi1 = early meiotic induction protein; MAD2 = mitotic arrest deficient 2 (spindle checkpoint protein); NEK = NIMA related kinase; NIMA = Nimrod A (drosophila gene).

Table 3. Top 10—GO Enrichment Analysis for the Overlap Gene Set

GO Name	GO Accession No.	FDR	Genes
Mitotic cell cycle	GO:0000278	1.08E-13	HELLS, DLGAP5, CCNB1, CENPE, ANLN, NUF2, CCNA2, CCNB2, MELK, PLK1, TPX2, PBK, BUB1, TYMS, CDKN3, FOXM1, HIST1H4K, RRM2, CENPF, ASPM, TTK, CEP55, STIL, KIF4A, KIF20A, CDC45, TOP2A
Mitotic cell cycle process	GO:1903047	1.08E-13	HELLS, DLGAP5, CCNB1, CENPE, ANLN, NUF2, CCNA2, CCNB2, MELK, PLK1, TPX2, PBK, BUB1, TYMS, CDKN3, FOXM1, RRM2, CENPF, ASPM, TTK, CEP55, STIL, KIF4A, KIF20A, CDC45, TOP2A
Mitotic nuclear division	GO:0007067	1.34E-11	MYBL2, HELLS, DLGAP5, CCNB1, CENPE, ANLN, NUF2, CCNA2, CCNB2, PLK1, TPX2, PBK, BUB1, CENPF, ASPM, CEP55, KIF4A, CDK1
Cell cycle process	GO:0022402	1.34E-11	FAP, ECT2, HELLS, DLGAP5, CCNB1, CENPE, ANLN, NUF2, CCNA2, CCNB2, MELK, TPX2, PBK, BUB1, TYMS, CDKN3, FOXM1, RRM2, CENPF, ASPM, MKI67, CEP55, STIL, KIF4A, KIF20A, CDC45, TOP2A
Cell division	GO:0051301	1.51E-11	ECT2, HELLS, CCNB1, KIF11, CENPE, ANLN, NUF2, CCNA2, BUB1B, CCNB2, PLK1, TPX2, BUB1, CENPF, ASPM, CEP55, KIF4A, KIF20A, CDK1, TOP2A
Nuclear division	GO:0000280	2.83E-11	MYBL2, HELLS, DLGAP5, CCNB1, CENPE, ANLN, NUF2, CCNA2, CCNB2, TPX2, PBK, BUB1, CENPF, ASPM, MKI67, CEP55, KIF4A, CDK1, TOP2A
Cell cycle	GO:0007049	4.37E-11	FAP, ECT2, HELLS, DLGAP5, CCNB1, CENPE, ANLN, NUF2, CCNA2, CCNB2, MELK, TPX2, PBK, BUB1, EXO1, TYMS, CDKN3, FOXM1, HIST1H4K, RRM2, CENPF, ASPM, MKI67, CEP55, STIL, KIF4A, KIF20A, CDC45, TOP2A
Spindle	GO:0005819	1.21E-9	ECT2, DLGAP5, CCNB1, KIF11, CENPE, BUB1B, PLK1, TPX2, CKAP2L, CENPF, ASPM, TTK, KIF4A, KIF20A, CDK1
Mitotic cell-cycle phase transition	GO:0044772	8.75E-8	MYBL2, CCNB1, CCNA2, BUB1B, CCNB2, MELK, PLK1, TYMS, CDKN3, FOXM1, RRM2, CENPF, CDK1, CDC45
Midbody	GO:0030496	1.33E-7	ECT2, CENPE, PLK1, CENPF, ASPM, CEP55, KIF4A, KIF20A, CDK1, SLC2A1

Definition of abbreviation: GO = Gene Ontology.

ATII Cells Exhibit Proliferative Capacity in Lung Fibrosis, Which Is Associated with Increased ECT2 Expression

Our functional annotation analysis implied a strong enrichment of cell cycle-associated pathways and proliferation in fibrotic ATII cells. We have previously reported that fibrotic ATII cells exhibit an increased proliferative capacity (41). Thus, we examined changes in the cell cycle of primary ATII cells that were isolated from Bleo- and PBS-treated mice, stained with propidium iodide, and analyzed by flow cytometry (Figure 5A). ATII cells from PBS-treated control mice were mainly found to be in the G0/G1 cell cycle phase (Figure 5B; percentage of total cells G0/G1: PBS 88.87% ± 2.41% vs. Bleo 79.91% ± 1.73%; ****P* < 0.001), whereas the amount of ATII cells from Bleo-treated mice was significantly increased in the S cell cycle phase (Figure 5B; percentage of total cells S: PBS 3.22% ± 1.71% vs. Bleo 7.53% ± 2.08%; ***P* < 0.01) and in the G2/M cell cycle phase (Figure 5B; percentage of total cells G2/M: PBS 7.91% ± 1.49% vs. Bleo 12.57% ± 0.81%; ***P* < 0.01). In addition, this finding was further supported by

Western blotting, which showed significantly higher protein levels of the cell proliferation marker Cyclin D1 (CCND1) in freshly isolated ATII cells from Bleo-treated mice compared to PBS (Figures 5C and 5D; relative protein level CCND1: PBS 0.49 ± 0.13 vs. Bleo 0.85 ± 0.31; **P* < 0.05). Immunohistochemical stainings of serial sections from IPF lung specimens for ECT2 and the cell proliferation marker proliferating cell nuclear antigen showed a colocalization PCNA in ATII cells *in situ* (Figure 5E, black arrows; compare with Figure 4D). Importantly, we observed that ECT2 was primarily localized in the cytoplasm, where it is known to be activated by phosphorylation and participates in the G2/M cell cycle phase (26, 42). Taken together, these data indicate that ECT2 contributes to a hyperplastic, proliferative capacity of fibrotic ATII cells.

ECT2 Knockdown Decreases the Proliferative Capacity of Fibrotic ATII Cells and Influences the Expression of Collagen Type I

To further assess the effect of ECT2 on ATII cell function in lung fibrosis, we performed

siRNA-mediated *Ect2* knockdown in primary ATII cells. A significant decrease of *Ect2* mRNA levels was observed after 24 hours of knockdown compared with scrambled (Scr) control in fibrotic pmATII cells (Figure 6A; ΔCt *Ect2*: siScr 24 h 1.26 ± 2.05 vs. siEct2 24 h -0.73 ± 1.34; **P* < 0.05). Western blotting confirmed the successful siRNA-mediated knockdown of ECT2 after 48 hours (Figure 6C; relative protein level ECT2: siScr 48 h 100.00 ± 0.00 vs. siEct2 48 h 6.98 ± 5.72; ****P* < 0.001) and 72 hours of transfection (Figures 6B and 6C; relative protein level ECT2: siScr 72 h 100.00 ± 0.00 vs. siEct2 72 h 5.07 ± 2.14; ****P* < 0.001). Similar results were obtained in healthy pmATII cells (data not shown). We analyzed the impact of decreased ECT2 expression on the proliferative capacity of fibrotic ATII cells by performing a 5-ethynyl-2'-deoxyuridine (EdU) assay and flow cytometry analysis (Figure 6D). The knockdown of *Ect2* significantly reduced the proliferative capacity of fibrotic ATII cells (Figure 6E; percentage of EdU⁺ cells: siScr 36.93% ± 4.02% vs. siEct2 23.03% ± 6.59%; **P* < 0.05; similar results were obtained in healthy pmATII cells [data not shown]). In

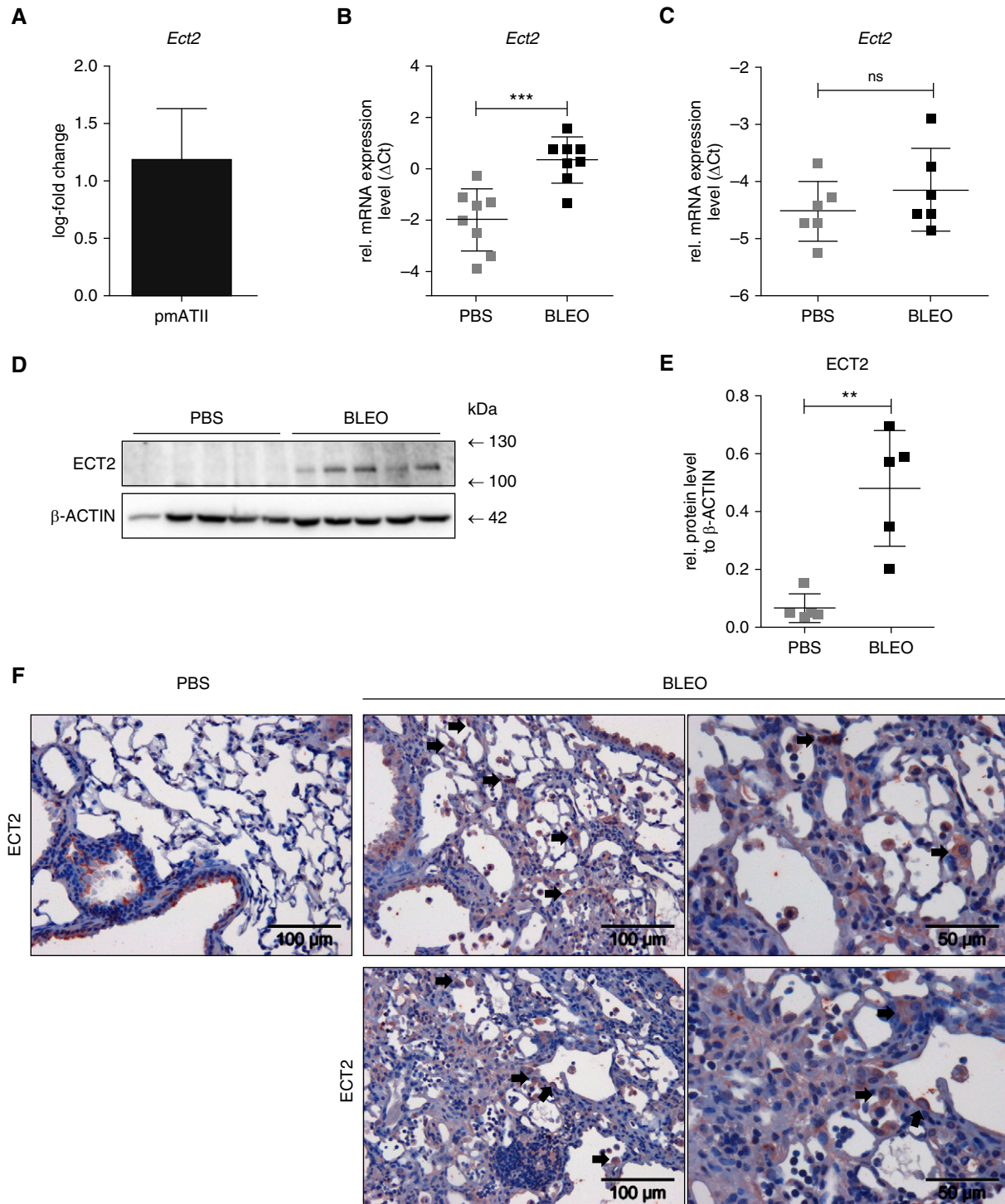


Figure 3. The oncogene ECT2 (epithelial cell transforming sequence 2) is upregulated in ATII cells from bleomycin (Bleo)-induced lung fibrosis. (A) Expression data for *Ect2* extracted from the pmATII microarray (41) presented as log₂ fold change of gene expression (Bleo-control; $n = 6$). (B) qRT-PCR for *Ect2* gene expression in freshly isolated pmATII cells from Bleo- and PBS-treated mice on Day 14 after treatment ($n = 8$). Expression data were normalized to *Hprt* and are presented as Δ Ct. (C) Gene expression of *Ect2* in whole-lung homogenates from Bleo- and PBS-treated mice on Day 14 after treatment ($n = 6$) assessed by qRT-PCR. Expression data were normalized to *Hprt* and are presented as Δ Ct. (D) Western blot data and (E) the respective quantification of ECT2 protein levels in freshly isolated pmATII cells from Bleo- and PBS-treated mice on Day 14 after treatment ($n = 5$). β -Actin served as the loading control. (F) Representative images of immunohistochemical staining for ECT2 in lung tissue from Bleo- and PBS-treated mice on Day 14 after treatment. Black arrows indicate ECT2⁺ hyperplastic ATII cells. Scale bars: 100 μ m and 50 μ m. All data are presented as mean \pm SD. Significance was determined using the unpaired *t*-test. Significance: ** $P < 0.01$ and *** $P < 0.001$. ns = nonsignificant; rel. = relative.

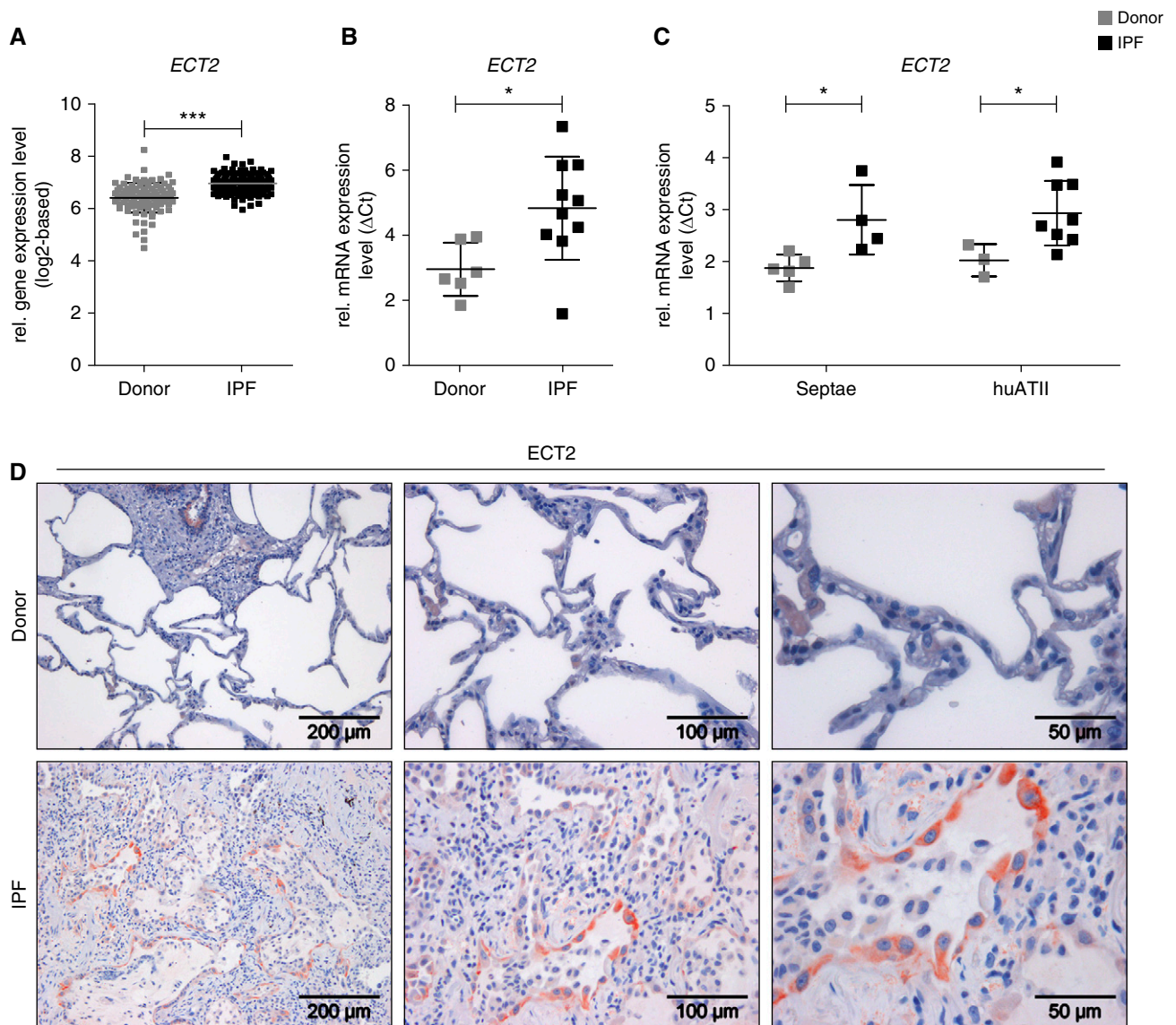


Figure 4. *ECT2* expression is increased in IPF and localized to hyperplastic alveolar epithelium. (A) *ECT2* expression data were extracted from the IPF microarray dataset (GSE47460) for IPF ($n = 121$) and donor ($n = 91$) samples as log₂-based expression values. (B) The gene expression of *ECT2* was assessed by qRT-PCR for total RNA extracted from whole-lung homogenates from IPF ($n = 10$) and donor ($n = 6$) lung tissue specimens. Expression data were normalized to *HPRT* and are presented as ΔCt. (C) qRT-PCR for *ECT2* gene expression levels in microdissected alveolar septae from IPF ($n = 4$) and donor ($n = 5$) lung tissue, as well as in freshly isolated primary human ATII (huATII) cells from IPF ($n = 8$) and donor ($n = 3$) lung specimens. Gene expression was normalized to *HPRT* and is presented as ΔCt values. (D) Representative images of immunohistochemical staining for *ECT2* in human IPF and donor lung tissue specimens. Scale bars: 200 μm, 100 μm, and 50 μm. All data are presented as mean ± SD. Significance was determined using the unpaired *t*-test. Significance: * $P < 0.05$ and *** $P < 0.001$.

addition, several recent reports from other investigators and us support the notion that reprogrammed, fibrotic ATII cells can contribute to ECM marker expression and deposition (41, 43). In line with this, we observed a significant decrease of the mesenchymal marker collagen type I (COL1) in fibrotic ATII cells after 48 hours (Figure 6C; relative protein level COL1: siScr 48 h 100.00 ± 0.00 vs. siEct2 48 h

56.58 ± 27.29; * $P < 0.05$) and 72 hours of *Ect2* knockdown (Figures 6B and 6C; relative protein level COL1: siScr 72 h 100.00 ± 0.00 vs. siEct2 72 h 39.67 ± 14.23; ** $P < 0.01$). Taken together, these results provide evidence that increased *ECT2* expression in fibrotic ATII cells contributes to distorted ATII cell reprogramming in IPF, including cell hyperplasia and ECM expression.

Discussion

IPF is a devastating lung disease with a fatal prognosis and a median survival of only 2.5–3.5 years (21). A recent meta-analysis by Whittaker Brown and colleagues demonstrated that IPF is an independent risk factor for lung cancer (44), and lung cancer further decreases survival in patients with IPF (45, 46). NSCLC commonly

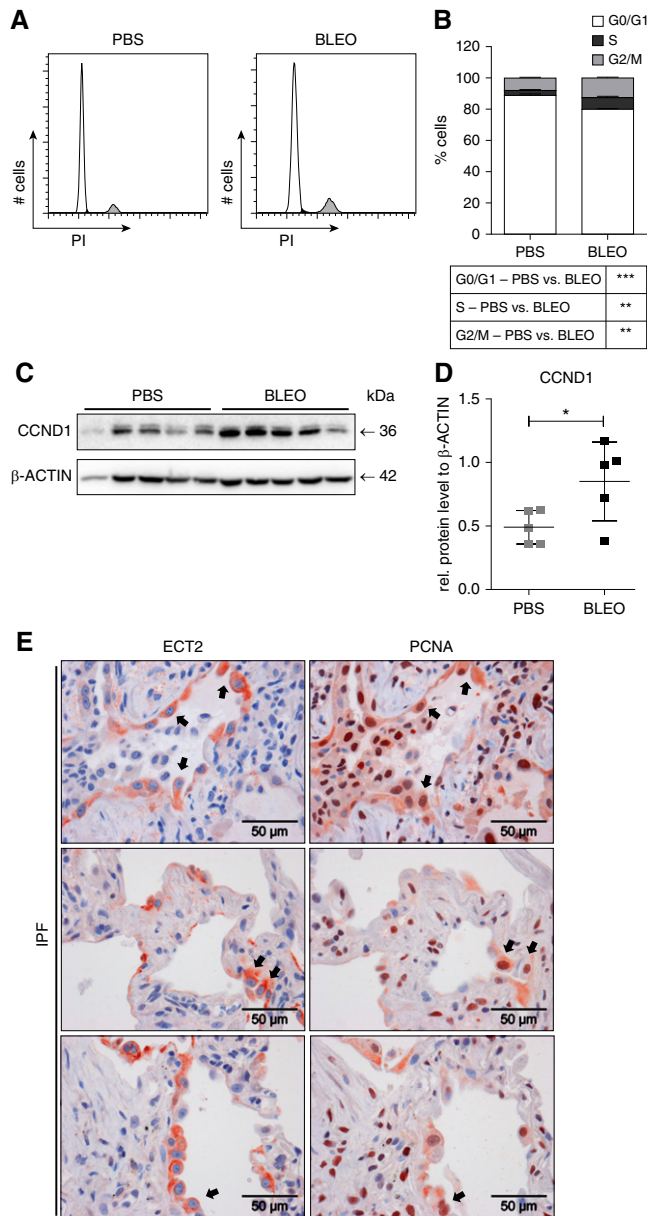


Figure 5. Enhanced ATII cell proliferation in lung fibrosis, associated with increased ECT2 expression. (A) Freshly isolated primary ATII cells from Bleo- and PBS-treated mice on Day 14 after treatment were stained with propidium iodide (PI) and analyzed by flow cytometry to assess cell cycle distribution ($n = 4$). (B) Cell cycle distribution was quantified using the FlowJo univariate cell cycle analysis algorithm and is presented as the percentage of cells in each cell cycle phase for Bleo and PBS, respectively. The total number of cells analyzed was set as 100%. Means of the cell cycle phases were compared using one-way ANOVA with Bonferroni's multiple-comparison post test. (C) Representative Western blot of CCND1 protein levels in freshly isolated pmATII cells from Bleo- and PBS-treated mice on Day 14 after administration and (D) the respective quantification of five independent experiments ($n = 5$). β -Actin served as the loading control. The representative Western blot image of β -actin is also shown in Figure 3D; for further explanation, see the METHODS section in the data supplement. Means were compared using an unpaired t -test. (E) Representative images of immunohistochemical staining for ECT2 and cell proliferation marker proliferating cell nuclear antigen (PCNA) in serial sections from human IPF lung tissue specimens. The upper-left image (ECT2) is shown in Figure 4D and is presented again for comparison with its associated serial PCNA staining. Black arrows indicate matched alveolar epithelial cells with ECT2 and PCNA colocalized staining. Scale bars: 50 μ m. All data are presented as mean \pm SD. Significance: * $P < 0.05$, ** $P < 0.01$, and *** $P < 0.001$.

occurs in IPF in areas of lung fibrosis and honeycombing, implying a pathomechanistic connection between the two diseases (11, 47). Recent advancements in therapeutic options for IPF include pirfenidone, which when administered perioperatively showed a reduction of lung cancer surgery-related complications (48), and nintedanib, which was originally developed as an anticancer treatment (49, 50). Both drugs can lead to decelerated disease progression in IPF (51). However, more targeted and effective therapies are needed. Here, we aimed to identify novel therapeutic targets by analyzing common gene expression patterns in IPF and NSCLC, and specifically investigated a potential role of the oncogene ECT2 in IPF.

IPF and NSCLC have been shown to share similar alterations in the expression levels of single genes, impacting their respective pathogenesis. For example, upregulation of epidermal growth factor receptor has been reported to occur in the lung epithelium of patients with IPF and to be negatively correlated with lung function parameters for disease severity (52), and increased levels of epidermal growth factor receptor in NSCLC have been shown to stimulate tumor development (53). Similar findings of aberrant gene expression have been reported for various other genes, including members of the WNT/ β -catenin pathway (54), transforming growth factor β 1 (55), Syndecan-2 (56, 57), and several matrix metalloproteinases (25). Here, we performed a systematic comparison of gene expression profiling datasets for IPF and NSCLC, and applied GSEA to investigate DEGs from three independent NSCLC gene expression profiling datasets for their enrichment in a large IPF dataset. Our GSEA revealed a common pattern of misregulated genes for both diseases, many of which are related to epithelial cell hyperplasia and proliferation. To minimize the probability of reporting a random selection of genes, we demonstrated functional enrichment in cell cycle-associated processes and increased protein-protein interactions, supporting the specificity and importance of our gene set. Of note, using a similar approach, Spek and Duitman recently performed a direct comparison of DEGs in IPF and lung cancer (non-GSEA based), and although the authors focused on the differences in IPF and NSCLC gene expression in that

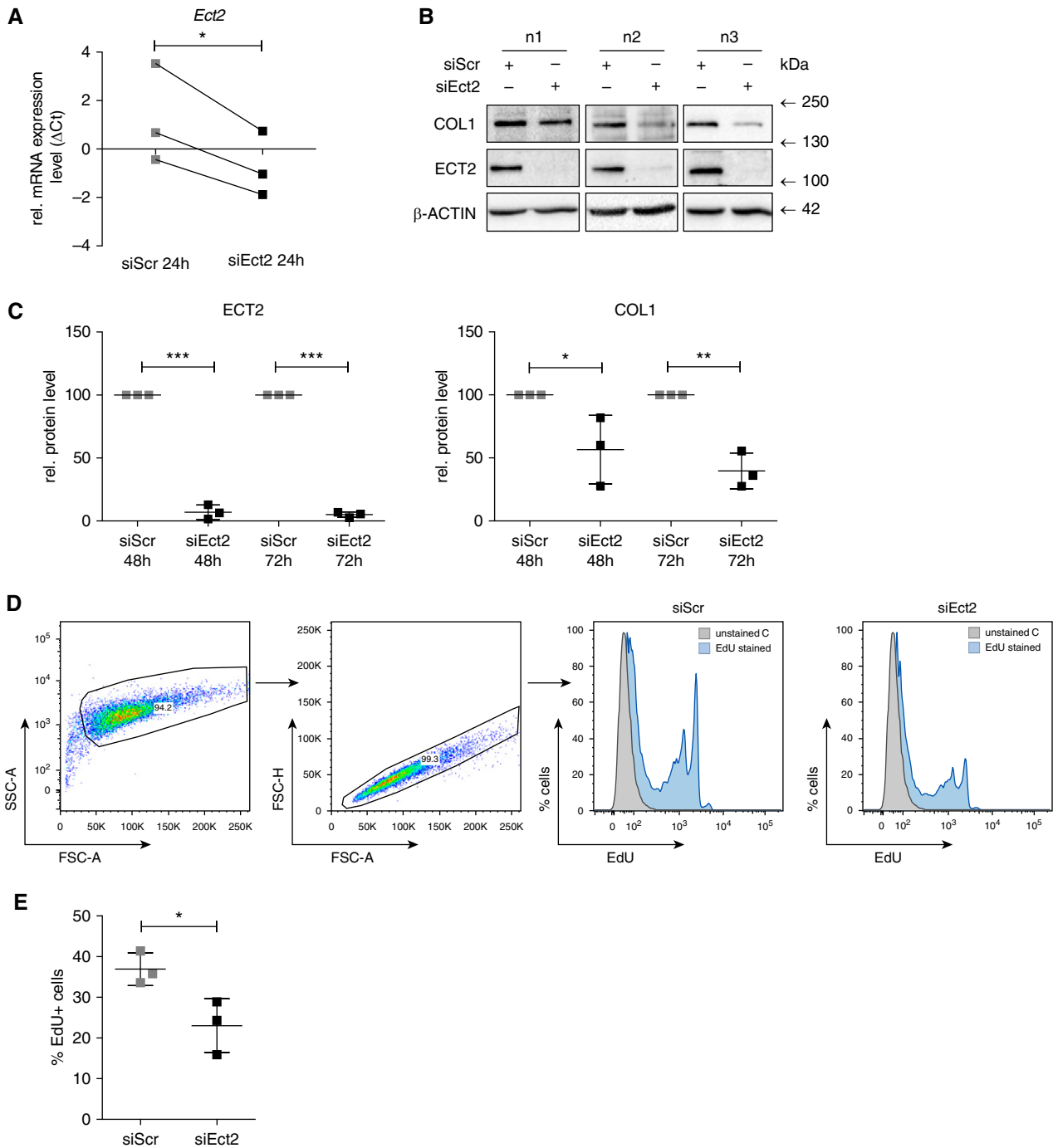


Figure 6. Transient knockdown of ECT2 decreases the proliferative capacity of ATII cells from experimental lung fibrosis and the expression of collagen type I (COL1). (A) Primary ATII cells were isolated from untreated wild-type mice, kept in cell culture for 2 days, and subsequently transfected with *Ect2* siRNAs or scrambled siRNA for 24 hours ($n = 3$). qRT-PCR for *Ect2* gene expression was performed. Expression data were normalized to *Hprt* and are presented as Δ Ct values. Significance was determined using the paired *t*-test. (B) Primary ATII cells were isolated from Bleo-treated mice on Day 14 after the instillation, kept in cell culture for 2 days, and subsequently transfected with *Ect2* siRNAs or scrambled siRNA for 48 hours and 72 hours ($n = 3$). Representative Western blot data (72 h; $n = 3$) and (C) corresponding quantifications of ECT2 and COL1 protein levels for 48 hours and 72 hours, respectively. Protein levels were normalized to scrambled control, which was set as 100%. β -Actin served as the loading control. Significance was determined using one-way ANOVA for repeated measures with Bonferroni's multiple-comparison post test. (D) pmATII cells were isolated from Bleo-treated mice on Day 14 after instillation, kept in cell culture for 2 days, and subsequently transfected with *Ect2* siRNAs or scrambled siRNA for 72 hours ($n = 3$). A 5-ethynyl-2'-deoxyuridine (EdU) assay was performed and EdU⁺ cells were recorded by flow cytometry. (E) Quantification of EdU⁺ cells ($n = 3$). Means were compared using the paired *t*-test. All data are presented as mean \pm SD. Significance: * $P < 0.05$, ** $P < 0.01$, and *** $P < 0.001$. FSC-A = forward scatter area; SSC-A = side scatter area.

study, they also noticed a functional correlation of the upregulated DEGs, and reasoned that drugs targeting those genes might be developed for IPF treatment (58).

Our identified subset of 92 genes showed a significant enrichment among the genes that were upregulated in ATII cells derived from IPF, as well as from Bleo-induced lung fibrosis in mice. In contrast, there was a negative enrichment in the IPF fibroblast dataset. Given that the cell of origin for NSCLC is a lung epithelial cell (59), these results might be largely driven by the fact that the input lists were generated from NSCLC data sets. However, the strong enrichment in IPF further supports the hypothesis that lung epithelial cells are important key driver cells in IPF. ATII cells are known to be progenitor cells that can differentiate into ATI cells (59), and within the distal lung ATII cells can undergo phenotypic changes and exhibit several abnormalities during fibrogenesis, which are referred to as “reprogramming” based on a recent National Heart, Lung, and Blood Institute Workshop report (18). These phenotypes include ATII cell hyperplasia and proliferation, as well as the ability to express mesenchymal marker proteins (60), which has also been observed in lung cancer (61). Correspondingly, we observed a functional enrichment of our gene set in cell cycle-associated processes and pathways. We further confirmed a significantly increased proliferative capacity of fibrotic ATII cells *in vitro*, which is in line with our own and other previous reports (41, 62, 63). Several recent *in vivo* studies demonstrated that targeting of ATII cell dysfunction, including epithelial cell proliferation, is an effective therapeutic approach in lung fibrosis (41, 64–66). A recent study demonstrated the potential impact of altered alveolar epithelial cell proliferation on IPF progression by limiting proliferation via DCK (deoxycytidine kinase) pathway inhibition, which resulted in reduced lung fibrosis (67). Similar results were obtained via inhibition of DDAH (dimethylarginine dimethylaminohydrolase) (64), as well as WISP1 (WNT1-inducible signaling pathway protein 1) (41). However, the mechanisms by which

these hyperproliferative ATII cells are connected to the progression of IPF pathogenesis is still not completely understood.

ECT2 is a GEF for the Rho family GTPases Cdc42, Rac1, and RhoA (26). ECT2 is an oncogene and the ECT2 gene is located on chromosome 3q26, which is a region that exhibits frequent genetic changes in various forms of cancer (68). Notably, this chromosomal region has also been associated with gene variants related to IPF, such as TERC (3q26) (69). ECT2 upregulation has been shown in different tumor types and is associated with the development of lung (27, 28, 70), breast (71), esophageal (72), and ovarian (73) cancer. The intracellular localization of ECT2 changes during the different cell cycle phases, as it switches from an inactive nuclear form during the interphase to a cytoplasmic form in the G2/M cell cycle phase, where it becomes activated by phosphorylation and participates in cytokinesis (26, 42). Hence, the intracellular localization of ECT2 is essential for its function, and although some studies have reported a nuclear mechanism of ECT2 underlying its role in cancer progression (73), others have shown that a cytoplasmic shift and subsequent activation of ECT2 drive tumor growth in NSCLC (27). Besides cytokinesis, ECT2 has been shown to support tumor growth, invasion, and epithelial–mesenchymal transition in NSCLC (27, 74). Our data demonstrate that ECT2 is upregulated in ATII cells in experimental and human lung fibrosis. Furthermore, we observed prominent, cytoplasmic ECT2 staining in the hyperplastic alveolar epithelium of IPF lung tissue *in situ*, indicating that similar to what has been reported for NSCLC, ECT2 is active in IPF. Furthermore, the transient knockdown of ECT2 resulted in a significantly reduced proliferative capacity of fibrotic ATII cells, further indicating that ECT2 expression is involved in fibrotic ATII cell hyperplasia and proliferation as observed in lung fibrosis. Interestingly, the KEGG pathway enrichment analysis for the Overlap gene set also revealed an enrichment of cellular senescence, and

oncogene-induced senescence has been reported to foster the formation of lung cancer (75). In addition, ATII cell senescence has also been demonstrated to be a feature of ATII cell reprogramming in IPF (6, 76). The potential transition from a proliferative to a senescent phenotype is of particular interest with regard to ECT2, as siRNA-mediated knockdown of ECT2 was identified in an extensive screen as an activator of senescent phenotypes (77).

Finally, there is the increasing notion that upon lung injury and fibrosis, ATII cells are able to produce and secrete ECM proteins, including collagens (41, 43). COL1 is one of the most common collagens in the lung and is highly regulated in IPF. Yang and colleagues demonstrated that the deletion of COL1 in activated alveolar epithelial cells from experimental lung fibrosis led to an attenuated fibrotic phenotype (43). Similarly, here we found COL1 expression in fibrotic ATII cells *in vitro*, which was significantly reduced upon ECT2 knockdown in fibrotic ATII cells. Additional studies to elucidate the precise cellular mechanisms by which ECT2 drives hyperplastic, proliferative ATII cells in IPF and whether these are linked to changes in ECM expression by ATII cells are required.

In summary, we have demonstrated that IPF and NSCLC share a common signature of misregulated genes associated with a fibrotic ATII cell phenotype. The ECT2 oncogene was identified as a strongly increased oncogene in IPF that contributed to ATII cell reprogramming *in vitro*. Thus, modulation of ECT2 *in vivo* will be required in future studies to advance our knowledge about a potential therapeutic role of ECT2-induced epithelial cell proliferation in IPF. ■

Author disclosures are available with the text of this article at www.atsjournals.org.

Acknowledgment: The authors thank all members of the Königshoff laboratory for stimulating discussions, and Julia Kipp and Anastasia van den Berg for excellent technical assistance. They also thank James DeGregori for thoroughly reading the manuscript and providing his input.

References

- Ley B, Collard HR, King TE Jr. Clinical course and prediction of survival in idiopathic pulmonary fibrosis. *Am J Respir Crit Care Med* 2011;183:431–440.
- Siegel RL, Miller KD, Jemal A. Cancer statistics, 2018. *CA Cancer J Clin* 2018;68:7–30.
- Baumgartner KB, Samet JM, Stidley CA, Colby TV, Waldron JA. Cigarette smoking: a risk factor for idiopathic pulmonary fibrosis. *Am J Respir Crit Care Med* 1997;155:242–248.
- Alberg AJ, Brock MV, Samet JM. Epidemiology of lung cancer: looking to the future. *J Clin Oncol* 2005;23:3175–3185.
- Samet JM. Does idiopathic pulmonary fibrosis increase lung cancer risk? *Am J Respir Crit Care Med* 2000;161:1–2.
- Lehmann M, Korfei M, Mutze K, Klee S, Skronska-Wasek W, Alsafadi HN, et al. Senolytic drugs target alveolar epithelial cell function and attenuate experimental lung fibrosis *ex vivo*. *Eur Respir J* 2017;50:1602367.
- Raghu G, Weycker D, Edelsberg J, Bradford WZ, Oster G. Incidence and prevalence of idiopathic pulmonary fibrosis. *Am J Respir Crit Care Med* 2006;174:810–816.
- Jung HI, Park JS, Lee M-Y, Park B, Kim HJ, Park SH, et al. Prevalence of lung cancer in patients with interstitial lung disease is higher than in those with chronic obstructive pulmonary disease. *Medicine (Baltimore)* 2018;97:e0071.
- Kato E, Takayanagi N, Takaku Y, Kagiya N, Kanauchi T, Ishiguro T, et al. Incidence and predictive factors of lung cancer in patients with idiopathic pulmonary fibrosis. *ERJ Open Res* 2018;4:00111–2016.
- Raghu G, Amatto VC, Behr J, Stowasser S. Comorbidities in idiopathic pulmonary fibrosis patients: a systematic literature review. *Eur Respir J* 2015;46:1113–1130.
- Tomassetti S, Gurioli C, Ryu JH, Decker PA, Ravaglia C, Tantalocco P, et al. The impact of lung cancer on survival of idiopathic pulmonary fibrosis. *Chest* 2015;147:157–164.
- Ozawa Y, Suda T, Naito T, Enomoto N, Hashimoto D, Fujisawa T, et al. Cumulative incidence of and predictive factors for lung cancer in IPF. *Respirology* 2009;14:723–728.
- Lee T, Park JY, Lee HY, Cho Y-J, Yoon HI, Lee JH, et al. Lung cancer in patients with idiopathic pulmonary fibrosis: clinical characteristics and impact on survival. *Respir Med* 2014;108:1549–1555.
- Liu Y, Zhu M, Geng J, Ban C, Zhang S, Chen W, et al. Incidence and radiologic-pathological features of lung cancer in idiopathic pulmonary fibrosis. *Clin Respir J* 2018;12:1700–1705.
- Guyard A, Danel C, Théou-Anton N, Debray M-P, Gibault L, Mordant P, et al. Morphologic and molecular study of lung cancers associated with idiopathic pulmonary fibrosis and other pulmonary fibroses. *Respir Res* 2017;18:120.
- Watanabe A, Miyajima M, Mishina T, Nakazawa J, Harada R, Kawaharada N, et al. Surgical treatment for primary lung cancer combined with idiopathic pulmonary fibrosis. *Gen Thorac Cardiovasc Surg* 2013;61:254–261.
- Kreuter M, Ehlers-Tenenbaum S, Schaaf M, Oltmanns U, Palmowski K, Hoffmann H, et al. Treatment and outcome of lung cancer in idiopathic interstitial pneumonias. *Sarcoidosis Vasc Diffuse Lung Dis* 2015;31:266–274.
- Blackwell TS, Tager AM, Borok Z, Moore BB, Schwartz DA, Anstrom KJ, et al. Future directions in idiopathic pulmonary fibrosis research: an NHLBI workshop report. *Am J Respir Crit Care Med* 2014;189:214–222.
- Richeldi L, Collard HR, Jones MG. Idiopathic pulmonary fibrosis. *Lancet* 2017;389:1941–1952.
- Selman M, Pardo A. Revealing the pathogenic and aging-related mechanisms of the enigmatic idiopathic pulmonary fibrosis: an integral model. *Am J Respir Crit Care Med* 2014;189:1161–1172.
- King TE Jr, Pardo A, Selman M. Idiopathic pulmonary fibrosis. *Lancet* 2011;378:1949–1961.
- Wistuba II, Gazdar AF. Lung cancer preneoplasia. *Annu Rev Pathol* 2006;1:331–348.
- Rabinovich EI, Kapetanaki MG, Steinfeld I, Gibson KF, Pandit KV, Yu G, et al. Global methylation patterns in idiopathic pulmonary fibrosis. *PLoS One* 2012;7:e33770.
- Carpagnano GE, Lacedonia D, Soccio P, Caccavo I, Patricelli G, Foschino Barbaro MP. How strong is the association between IPF and lung cancer? An answer from airway's DNA. *Med Oncol* 2016;33:119.
- Königshoff M. Lung cancer in pulmonary fibrosis: tales of epithelial cell plasticity. *Respiration* 2011;81:353–358.
- Tatsumoto T, Xie X, Blumenthal R, Okamoto I, Miki T. Human ECT2 is an exchange factor for Rho GTPases, phosphorylated in G2/M phases, and involved in cytokinesis. *J Cell Biol* 1999;147:921–928.
- Justilien V, Fields AP. Ect2 links the PKC α -Par6 α complex to Rac1 activation and cellular transformation. *Oncogene* 2009;28:3597–3607.
- Hirata D, Yamabuki T, Miki D, Ito T, Tsuchiya E, Fujita M, et al. Involvement of epithelial cell transforming sequence-2 oncoantigen in lung and esophageal cancer progression. *Clin Cancer Res* 2009;15:256–266.
- Ulke H, Mutze K, Wagner D, Stein MM, Lindner M, Behr J, et al. Non-small cell lung cancer (NSCLC) gene signature in idiopathic pulmonary fibrosis (IPF) [abstract]. *Am J Respir Crit Care Med* 2017;195:A2408.
- Edgar R, Domrachev M, Lash AE. Gene Expression Omnibus: NCBI gene expression and hybridization array data repository. *Nucleic Acids Res* 2002;30:207–210.
- Silvester N, Alako B, Amid C, Cerdeño-Tarraga A, Clarke L, Cleland I, et al. The European Nucleotide Archive in 2017. *Nucleic Acids Res* 2018;46:D36–D40.
- Peng X, Moore M, Mathur A, Zhou Y, Sun H, Gan Y, et al. Plexin C1 deficiency permits synaptotagmin 7-mediated macrophage migration and enhances mammalian lung fibrosis. *FASEB J* 2016;30:4056–4070.
- Bauer Y, Tedrow J, de Bernard S, Birker-Robaczewska M, Gibson KF, Guardela BJ, et al. A novel genomic signature with translational significance for human idiopathic pulmonary fibrosis. *Am J Respir Cell Mol Biol* 2015;52:217–231.
- Yang IV, Coldren CD, Leach SM, Seibold MA, Murphy E, Lin J, et al. Expression of cilium-associated genes defines novel molecular subtypes of idiopathic pulmonary fibrosis. *Thorax* 2013;68:1114–1121.
- Kadara H, Fujimoto J, Yoo S-Y, Maki Y, Gower AC, Kabbout M, et al. Transcriptomic architecture of the adjacent airway field cancerization in non-small cell lung cancer. *J Natl Cancer Inst* 2014;106:dju004.
- Kabbout M, Garcia MM, Fujimoto J, Liu DD, Woods D, Chow C-W, et al. ETS2 mediated tumor suppressive function and MET oncogene inhibition in human non-small cell lung cancer. *Clin Cancer Res* 2013;19:3383–3395.
- Sanchez-Palencia A, Gomez-Morales M, Gomez-Capilla JA, Pedraza V, Boyero L, Rosell R, et al. Gene expression profiling reveals novel biomarkers in nonsmall cell lung cancer. *Int J Cancer* 2011;129:355–364.
- Vuga LJ, Ben-Yehudah A, Kovkarova-Naumovski E, Oriss T, Gibson KF, Feghali-Bostwick C, et al. WNT5A is a regulator of fibroblast proliferation and resistance to apoptosis. *Am J Respir Cell Mol Biol* 2009;41:583–589.
- Xu Y, Mizuno T, Sridharan A, Du Y, Guo M, Tang J, et al. Single-cell RNA sequencing identifies diverse roles of epithelial cells in idiopathic pulmonary fibrosis. *JCI Insight* 2016;1:e90558.
- Subramanian A, Tamayo P, Mootha VK, Mukherjee S, Ebert BL, Gillette MA, et al. Gene set enrichment analysis: a knowledge-based approach for interpreting genome-wide expression profiles. *Proc Natl Acad Sci USA* 2005;102:15545–15550.
- Königshoff M, Kramer M, Balsara N, Wilhelm J, Amarie OV, Jahn A, et al. WNT1-inducible signaling protein-1 mediates pulmonary fibrosis in mice and is upregulated in humans with idiopathic pulmonary fibrosis. *J Clin Invest* 2009;119:772–787.
- Saito S, Liu X-F, Kamijo K, Raziuddin R, Tatsumoto T, Okamoto I, et al. Deregulation and mislocalization of the cytokinesis regulator ECT2 activate the rho signaling pathways leading to malignant transformation. *J Biol Chem* 2004;279:7169–7179.
- Yang J, Wheeler SE, Velikoff M, Kleaveland KR, LaFemina MJ, Frank JA, et al. Activated alveolar epithelial cells initiate fibrosis through secretion of mesenchymal proteins. *Am J Pathol* 2013;183:1559–1570.
- Whittaker Brown SA, Dobelle M, Padilla M, Agovino M, Wisnivesky JP, Hashim D, et al. Idiopathic pulmonary fibrosis and lung cancer: a systematic review and meta-analysis. *Ann Am Thorac Soc* 2019;16:1041–1051.

45. Mohamed S, Bayoumi H, El-Aziz NA, Mousa E, Gamal Y. Prevalence, risk factors, and impact of lung Cancer on outcomes of idiopathic pulmonary fibrosis: a study from the Middle East. *Multidiscip Respir Med* 2018;13:37.
46. Lee KJ, Chung MP, Kim YW, Lee JH, Kim K-S, Ryu JS, *et al.* Prevalence, risk factors and survival of lung cancer in the idiopathic pulmonary fibrosis. *Thorac Cancer* 2012;3:150–155.
47. Horowitz JC, Osterholzer JJ, Marazioti A, Stathopoulos GT. “Scar-cinoma”: viewing the fibrotic lung mesenchymal cell in the context of cancer biology. *Eur Respir J* 2016;47:1842–1854.
48. Iwata T, Yoshino I, Yoshida S, Ikeda N, Tsuboi M, Asato Y, *et al.*; West Japan Oncology Group. A phase II trial evaluating the efficacy and safety of perioperative pirfenidone for prevention of acute exacerbation of idiopathic pulmonary fibrosis in lung cancer patients undergoing pulmonary resection: West Japan Oncology Group 6711 L (PEOPLE Study). *Respir Res* 2016;17:90.
49. McCormack PL. Nintedanib: first global approval. *Drugs* 2015;75:129–139.
50. Chambers RC, Mercer PF. Mechanisms of alveolar epithelial injury, repair, and fibrosis. *Ann Am Thorac Soc* 2015;12:S16–S20.
51. Rogliani P, Calzetta L, Cavalli F, Matera MG, Cazzola M. Pirfenidone, nintedanib and N-acetylcysteine for the treatment of idiopathic pulmonary fibrosis: a systematic review and meta-analysis. *Pulm Pharmacol Ther* 2016;40:95–103.
52. Tzouveleakis A, Ntoliou P, Karameris A, Vilaras G, Boglou P, Koulelidis A, *et al.* Increased expression of epidermal growth factor receptor (EGF-R) in patients with different forms of lung fibrosis. *BioMed Res Int* 2013;2013:654354.
53. Xu N, Fang W, Mu L, Tang Y, Gao L, Ren S, *et al.* Overexpression of wildtype EGFR is tumorigenic and denotes a therapeutic target in non-small cell lung cancer. *Oncotarget* 2016;7:3884–3896.
54. McCrean PD, Gottardi CJ. Beyond β -catenin: prospects for a larger catenin network in the nucleus. *Nat Rev Mol Cell Biol* 2016;17:55–64.
55. Marwitz S, Depner S, Dvornikov D, Merkle R, Szczygiel M, Müller-Decker K, *et al.* Downregulation of the TGF β pseudoreceptor BAMBI in non-small cell lung cancer enhances TGF β signaling and invasion. *Cancer Res* 2016;76:3785–3801.
56. Shi Y, Gochuico BR, Yu G, Tang X, Osorio JC, Fernandez IE, *et al.* Syndecan-2 exerts antifibrotic effects by promoting caveolin-1-mediated transforming growth factor- β receptor I internalization and inhibiting transforming growth factor- β 1 signaling. *Am J Respir Crit Care Med* 2013;188:831–841.
57. Tsoyi K, Osorio JC, Chu SG, Fernandez IE, Poli S, Sholl L, *et al.* Lung adenocarcinoma syndecan-2 potentiates cell invasiveness. *Am J Respir Cell Mol Biol* 2019;60:659–666.
58. Spek CA, Duitman J. Is idiopathic pulmonary fibrosis a cancer-like disease? Transcriptome analysis to fuel the debate. *ERJ Open Res* 2019;5:00157–02018.
59. Desai TJ, Brownfield DG, Krasnow MA. Alveolar progenitor and stem cells in lung development, renewal and cancer. *Nature* 2014;507:190–194.
60. Willis BC, Liebler JM, Luby-Phelps K, Nicholson AG, Crandall ED, du Bois RM, *et al.* Induction of epithelial-mesenchymal transition in alveolar epithelial cells by transforming growth factor- β 1: potential role in idiopathic pulmonary fibrosis. *Am J Pathol* 2005;166:1321–1332.
61. Tsoukalas N, Aravantinou-Fatorou E, Tolia M, Giaginis C, Galanopoulos M, Kiakou M, *et al.* Epithelial-mesenchymal transition in non small-cell lung cancer. *Anticancer Res* 2017;37:1773–1778.
62. Akram KM, Lomas NJ, Forsyth NR, Spiteri MA. Alveolar epithelial cells in idiopathic pulmonary fibrosis display upregulation of TRAIL, DR4 and DR5 expression with simultaneous preferential over-expression of pro-apoptotic marker p53. *Int J Clin Exp Pathol* 2014;7:552–564.
63. Wei CH, Baratelli FE, Xiao G-Q, Koss MN, Elatre W. Evaluation of cyclin D1 as a discriminatory immunohistochemical biomarker for idiopathic pulmonary fibrosis. *Appl Immunohistochem Mol Morphol* 2019;27:e11–e15.
64. Pullamsetti SS, Savai R, Dumitrascu R, Dahal BK, Wilhelm J, Konigshoff M, *et al.* The role of dimethylarginine dimethylaminohydrolase in idiopathic pulmonary fibrosis. *Sci Transl Med* 2011;3:87ra53.
65. Bueno M, Lai Y-C, Romero Y, Brands J, St Croix CM, Kamga C, *et al.* PINK1 deficiency impairs mitochondrial homeostasis and promotes lung fibrosis. *J Clin Invest* 2015;125:521–538.
66. Yu G, Tzouveleakis A, Wang R, Herazo-Maya JD, Ibarra GH, Srivastava A, *et al.* Thyroid hormone inhibits lung fibrosis in mice by improving epithelial mitochondrial function. *Nat Med* 2018;24:39–49.
67. Weng T, Poth JM, Karmouty-Quintana H, Garcia-Morales LJ, Melicoff E, Luo F, *et al.* Hypoxia-induced deoxycytidine kinase contributes to epithelial proliferation in pulmonary fibrosis. *Am J Respir Crit Care Med* 2014;190:1402–1412.
68. Fields AP, Justilien V, Murray NR. The chromosome 3q26 OncCassette: a multigenic driver of human cancer. *Adv Biol Regul* 2016;60:47–63.
69. Fingerlin TE, Murphy E, Zhang W, Peljto AL, Brown KK, Steele MP, *et al.* Genome-wide association study identifies multiple susceptibility loci for pulmonary fibrosis. *Nat Genet* 2013;45:613–620.
70. Murata Y, Minami Y, Iwakawa R, Yokota J, Usui S, Tsuta K, *et al.* ECT2 amplification and overexpression as a new prognostic biomarker for early-stage lung adenocarcinoma. *Cancer Sci* 2014;105:490–497.
71. Wang H, Liang J, Zheng H, Xiao H. Expression and prognostic significance of ECT2 in invasive breast cancer. *J Clin Pathol* 2018;71:442–445.
72. Qixing M, Gaochao D, Wenjie X, Anpeng W, Bing C, Weidong M, *et al.* Microarray analyses reveal genes related to progression and prognosis of esophageal squamous cell carcinoma. *Oncotarget* 2017;8:78838–78850.
73. Huff LP, Decristo MJ, Trembath D, Kuan PF, Yim M, Liu J, *et al.* The role of Ect2 nuclear RhoGEF activity in ovarian cancer cell transformation. *Genes Cancer* 2013;4:460–475.
74. Tan H, Wang X, Yang X, Li H, Liu B, Pan P. Oncogenic role of epithelial cell transforming sequence 2 in lung adenocarcinoma cells. *Exp Ther Med* 2016;12:2088–2094.
75. Liu XL, Ding J, Meng LH. Oncogene-induced senescence: a double edged sword in cancer. *Acta Pharmacol Sin* 2018;39:1553–1558.
76. Disayabutr S, Kim EK, Cha S-I, Green G, Naikawadi RP, Jones KD, *et al.* miR-34 miRNAs regulate cellular senescence in type II alveolar epithelial cells of patients with idiopathic pulmonary fibrosis. *PLoS One* 2016;11:e0158367.
77. Cairney CJ, Godwin LS, Bilsland AE, Burns S, Stevenson KH, McGarry L, *et al.* A ‘synthetic-sickness’ screen for senescence re-engagement targets in mutant cancer backgrounds. *PLoS Genet* 2017;13:e1006942.